Two distinct modes of myosin assembly and dynamics during epithelial wound closure

Masako Tamada,[1] Tomas D. Perez,[2] W. James Nelson,[2] and Michael P. Sheetz[1]

[1]Department of Biological Sciences, Columbia University, New York, NY 10027
[2]Department of Biological Sciences and Molecular and Cellular Physiology, Stanford University, Stanford, CA 94305

Actomyosin contraction powers the sealing of epithelial sheets during embryogenesis and wound closure; however, the mechanisms are poorly understood. After laser ablation wounding of Madin–Darby canine kidney cell monolayers, we observed distinct steps in wound closure from time-lapse images of myosin distribution during resealing. Immediately upon wounding, actin and myosin II regulatory light chain accumulated at two locations: (1) in a ring adjacent to the tight junction that circumscribed the wound and (2) in fibers at the base of the cell in membranes extending over the wound site. Rho-kinase activity was required for assembly of the myosin ring, and myosin II activity was required for contraction but not for basal membrane extension. As it contracted, the myosin ring moved toward the basal membrane with ZO-1 and Rho-kinase. Thus, we suggest that tight junctions serve as attachment points for the actomyosin ring during wound closure and that Rho-kinase is required for localization and activation of the contractile ring.

Introduction

Cells show dynamic reorganization of cytoskeletons to migrate and change their shape. Recent studies have revealed similarities in signaling pathways and cytoskeletal reorganization involved in cell shape changes during epithelial tissue morphogenesis and wound healing (for review see Martin and Parkhurst, 2004). Nonmuscle myosin II is an actin-based motor protein and is presumed to contract the actin cytoskeleton. In higher eukaryotes, nonmuscle myosin II (hereafter referred to as myosin) assembly and motor activity are controlled by the phosphorylation of myosin regulatory light chain (MLC) at Thr18/Ser19 (Ikebe and Hartshorne, 1985).

Myosin is required for epithelial morphogenesis in *Drosophila melanogaster* (Young et al., 1993; Bertet et al., 2004; Nikolaidou and Barrett, 2004; Zallen and Wieschaus, 2004) and in *Caenorhabditis elegans* (Shelton et al., 1999). It is not clear, however, whether myosin is required as a motor to change cell shape, a regulator of cell–cell and cell–matrix adhesion, or a combination of both. Myosin also plays an important role during epithelial wound healing in which cell migration is coordinated with the purse string–like contraction of a thick cable of actin and myosin in the leading edge of marginal cells encompassing a large wound, drawing the wound edges together (Martin and Lewis, 1992; Bement et al., 1993; Wood et al., 2002). A purse string–like cable is also formed around dead cell remnants to extrude apoptosed cells (Rosenblatt et al., 2001). How the actomyosin contractile apparatus is formed and how it drives cytoskeletal rearrangement to cause closure of epithelial sheets are important questions.

To address these questions, we examined the sequence of steps involved during wound closure in MDCK cell sheets by using live-cell time-lapse imaging of the cell shape, myosin, and other associated proteins. Our observations identify a regulatory mechanism for localized assembly and activation of a myosin ring at the tight junction in cells surrounding the wound. Ring contraction can integrate neighboring cell shape changes and appears to cooperate with another myosin complex at the extending basal membrane.

Correspondence to Michael P. Sheetz: ms2001@columbia.edu

M. Tamada's present address is Kobe University Graduate School of Medicine, Chuo-ku, Kobe 650-0017 Hyogo, Japan.

T.D. Perez's present address is Department of Biological Sciences, Columbia University, New York, NY 10027.

Abbreviation used in this paper: MLC, myosin II regulatory light chain.

The online version of this article contains supplemental material.

Results and discussion

Rearrangement of cell–cell adhesions and cell shape changes during wound closure

To study both cell and protein dynamics during different stages of wound closure of an epithelial sheet, we reproducibly formed small, circular wounds in MDCK cell monolayers by laser

The Journal of Cell Biology, Vol. 176, No. 1, January 1, 2007 27–33
http://www.jcb.org/cgi/doi/10.1083/jcb.200609116

ablation (Kiehart et al., 2000) and performed live-cell time-lapse imaging during wound closure. After wounding, dead cell remnants were extruded from the wound site (Fig. S1 A, available at http://www.jcb.org/cgi/content/full/jcb.200609116/DC1), as reported previously (Rosenblatt et al., 2001). When we wounded a monolayer of MDCK cells expressing E-cadherin fused to red fluorescent protein (Ecad-RFP), Ecad-RFP fluorescence decreased at the plasma membrane between the wounded cell and surrounding cells 5–10 min after laser ablation, and Ecad-RFP at contacts between surrounding cells extended toward the center of the wound and eventually coalesced into a vertex between multiple cells (Fig. 1 A). These results show rearrangement of cell–cell adhesions occurring concomitantly with cell shape change during wound closure.

MLC assembly at two distinct sites and dynamics in wound closure

In addition to remodeling cell–cell adhesions, cell shape change involved dynamic rearrangement of the actin cytoskeleton. To define the sequence of steps that were involved in actomyosin assembly and movement to close the wound, we followed the dynamics of myosin localization using MLC fused to EGFP (MLC-EGFP). In confluent MDCK cell monolayers, MLC-EGFP was diffusely distributed in the cytoplasm and colocalized with F-actin fibers at the base of cells, but it was not localized to the boundary between cells either at the base of the cells or at lateral membranes (Fig. 1, B and E). After laser ablation, MLC-EGFP assembled into a ring in cells surrounding the wound, consistent with previous studies showing myosin localization around a wound in cell sheets and *D. melanogaster* embryos (Bement et al., 1993; Wood et al., 2002). This MLC ring contracted over time during wound closure (Fig. 1 B), as did an EGFP-actin ring assembled around the wound (Fig. S1 B; Rosenblatt et al., 2001; Wood et al., 2002).

Next, we analyzed MLC-EGFP distribution along the apical–basal axis during wound closure in time-lapse images of XZ sections (Fig. 1, C and D). About 5 min after laser ablation, MLC-EGFP fluorescence began to accumulate at the borders between the apical and lateral membranes and between the basal and lateral membranes (referred to as the apical–lateral border and basal–lateral border, respectively) of cells facing the wound. Both apical and basal MLC-EGFP moved toward the wound center. However, apical MLC-EGFP moved toward the basal cell membrane and eventually coalesced with basal MLC-EGFP at the base of cells (Fig. 1 D). Note that the shape of cells viewed in XZ sections changed from rectangular to triangular as the apical MLC-EGFP drew the upper edge inward and down to the base (Fig. 1 D). Thus, myosin movement tracked the closure of the wound, thinning adjacent cells to cover the wound.

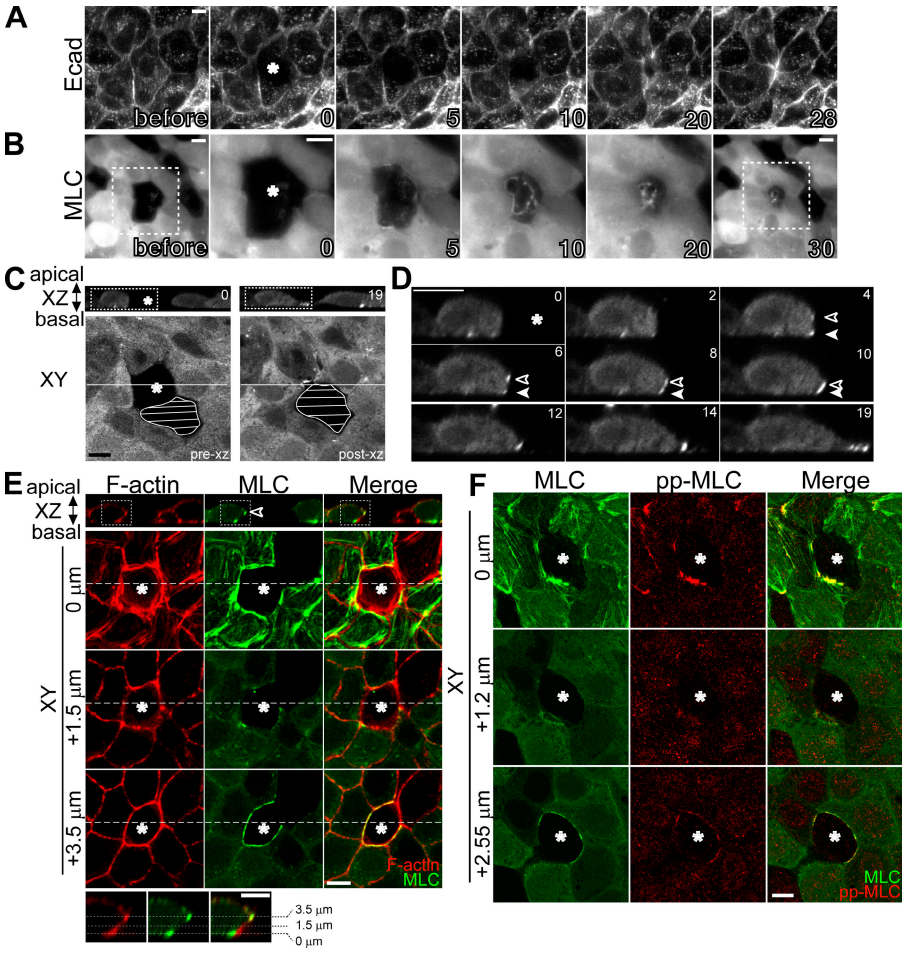

Figure 1. **The dynamics of MLC localization and cell shape changes during wound closure.** (A and B) One or two cells in a monolayer of MDCK cells expressing Ecad-RFP (A) or MLC-EGFP (B) were laser ablated. Epifluorescent images of cells were collected before and after laser ablation. Asterisks indicate the ablated cells. Elapsed time is indicated on each panel in minutes. Micrographs of 0, 5, 10, and 20 min in B show the images of the boxed region at higher magnification. (C) One cell in MLC-EGFP cell monolayer was laser ablated, and time-lapse XZ images of MLC-EGFP were collected for 19 min. XY sections were taken when XZ imaging was started (pre-xz) and finished (post-xz). White lines in XY sections indicate the position of XZ sections. Hatched regions represent cells with low MLC-EGFP. (D) Time-lapse images of the boxed region in C at higher magnification. MLC-EGFP accumulated at the apical–lateral border (open arrowheads) and basal–lateral border (closed arrowheads) of cells surrounding the ablated cell. (E) About 5 min after ablation, MLC-EGFP cells were fixed and F-actin was visualized with Alexa Fluor 568 phalloidin. The bottom panels show the images of the boxed regions at higher magnification. MLC-EGFP concentrated into a ring at the apical–lateral border and into fibers at the basal–lateral border with F-actin around wound. (F) Phospho-MLC accumulates around the wound. MLC-EGFP cells were treated and fixed as in E and stained with anti–phospho-MLC (Thr18/Ser19) antibody. Protein distributions are shown at three Z positions. Bars, 10 µm.

In cells fixed ~5 min after ablation, MLC-EGFP was concentrated in a ring around the wound, 3.5 μm above the base of the cells (Fig. 1 E). This MLC-EGFP ring corresponded to the accumulation of MLC-EGFP at the apical tip of the lateral membrane in XZ images (Fig. 1 D). The MLC- EGFP ring colocalized with F-actin identified by Alexa Fluor 568 phalloidin (Fig. 1 E). Basal XY sections of fixed cells also showed accumulation of MLC-EGFP fibers and F-actin around the wound (Fig. 1 E), and this MLC-EGFP accumulation appeared to correspond to the MLC-EGFP at the basal–lateral border in live cells (Fig. 1 D). An antibody specific for phospho-MLC (Thr18/Ser19) recognized both MLC at the apical–lateral and basal–lateral borders of cells surrounding the wound (Fig. 1 F). Thus, both actin and active myosin are present at the apical–lateral and basal–lateral borders, indicating a possible role of actomyosin contraction in wound closure.

These results indicate that MLC accumulated in two spatially distinct complexes: one at the basal–lateral border adjacent to cell extensions into the wound and the other in a ring at the apical–lateral border of cells around the wound. The ring structure descended from its initial apical position to a basal position as it contracted and constricted the lateral membrane of cells surrounding the wound, thereby expelling remnants of dead cells into the medium as the continuity of the monolayer was restored (see Fig. 5 B).

Myosin activity is required for contraction of the actomyosin ring and wound closure

We tested whether myosin activity was required to contract the ring and close the wound. In the presence of blebbistatin, a non-muscle myosin II ATPase inhibitor, MLC-EGFP accumulated at the apical–lateral and basal–lateral borders in cells surrounding the wound (Fig. 2 A). However, the MLC-EGFP ring did not contract, although the ring shape changed as cells extended into the wound from the basal membrane (Fig. 2 A b). Upon removal of blebbistatin, the MLC-EGFP ring began to contract and closed the wound within 5 min (Fig. 2 A). These results indicate that myosin is the motor providing the primary driving force to contract the MLC ring at the apical–lateral border but not to extend basal membranes into the wound and that ring contraction is required to constrict the lateral membrane of cells so that the cells closing the wound coalesce into a vertex.

Rho-kinase is involved in wound closure at both sites

MLC phosphorylation is critical for actomyosin assembly and contractility. Among kinases known to phosphorylate MLC, both myosin light chain kinase (MLCK) and Rho-associated kinase (Rho-kinase) have been linked to wound closure and extrusion of apoptotic cells (Rosenblatt et al., 2001; Russo et al., 2005). To examine their involvement in MLC accumulation at each site, we observed wound closure in the presence of their inhibitors. Y27632, a Rho-kinase inhibitor, inhibited formation of the MLC-EGFP ring at the apical–lateral border and subsequent contraction of the lateral membrane (Fig. 2 B). However, in the presence of Y27632, MLC-EGFP still accumulated at the basal–lateral border of cells around the wound even though actin stress fibers containing MLC-EGFP appeared mostly disrupted, and very thin basal cell membrane protrusions extended into the wound, partially closing it. However, at the level of the

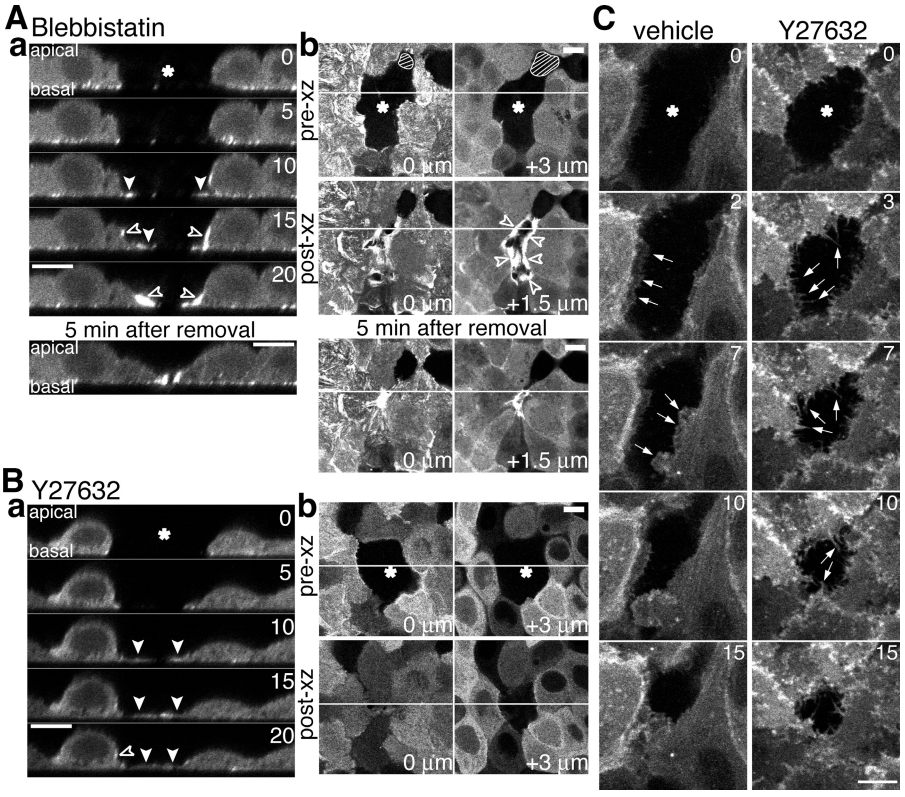

Figure 2. **Myosin activity is required for contraction of the actomyosin ring and wound closure, and Rho-kinase is involved in ring accumulation.** MLC-EGFP cells were treated with 50 μM blebbistatin for 20 min (A) or 20 μM Y27632 for 1 h (B) before laser ablation. After ablation, cells were observed for 20 min in the presence of inhibitors (a). (A) In the presence of blebbistatin, MLC-EGFP accumulated, but the wound remained open 20 min after laser ablation (open arrowheads). Basal membranes extended into the wound space (closed arrowheads). 5 min after removal of blebbistatin, the wound was closed (a and b, bottom). (B) In the presence of Y27632, the accumulation of MLC-EGFP at the apical–lateral border was attenuated (open arrowhead), but basal membranes extended into the wound space (closed arrowheads). (C) After ablation, the basal plane of EGFP-actin cells was observed. Cells extended into the wound site with lamellipodial protrusions (left, arrows), and these lamellipodial protrusions were replaced by filopodia in the presence of Y27632 (right, arrows). Asterisks indicate the ablated cells. Bars, 10 μm.

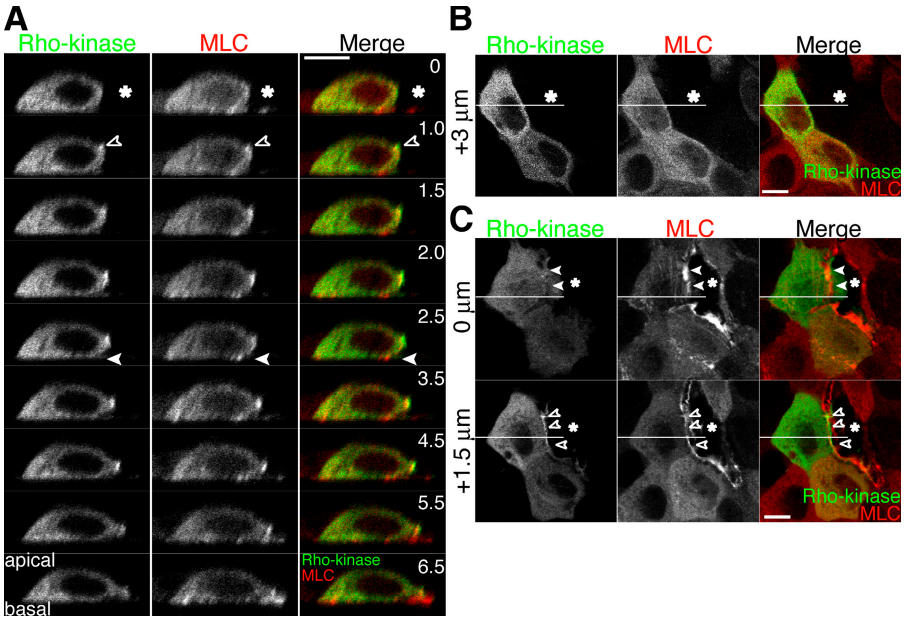

Figure 3. **Rho-kinase accumulates at the apical–lateral border of cells surrounding the wound.** (A) Cells in a monolayer of MLC-RFP cells transiently expressing EGFP–Rho-kinase were ablated, and XZ images were collected. (B and C) XY images were taken before (B) and after (C) XZ imaging. EGFP–Rho-kinase and MLC-RFP coaccumulated simultaneously at the apical–lateral border (open arrowheads). EGFP–Rho-kinase did not accumulate at the basal–lateral border (closed arrowheads). Asterisks indicate the ablated cells. Bars, 10 µm.

apical–lateral border, the wound space remained open (Fig. 2 B). ML-7, an MLCK inhibitor, had little or no effect on either MLC-EGFP accumulation or the ensuing cell shape changes in our system (Fig. S2, available at http://www.jcb.org/cgi/content/full/jcb.200609116/DC1).

To determine the structure of the basal membrane protrusions in the XY plane, we analyzed cells expressing EGFP-actin. We found that cells extended lamellipodial protrusions into the wound site. However, in the presence of Y27632, lamellipodial protrusions were replaced by filopodia (Fig. 2 C). These results indicate that Rho-kinase is involved in actomyosin organization at both sites. At the apical–lateral border, Rho-kinase is required for assembling the MLC ring and the following changes in cell shape during ring contraction. At the basal–lateral border, Rho-kinase is required to activate lamellipodial protrusion and maintain its morphology. The mechanism for MLC accumulation at the basal–lateral border is unknown. Because MLC accumulation was inhibited at both sites in cells expressing C3 toxin (unpublished data), both accumulations appear to be Rho dependent.

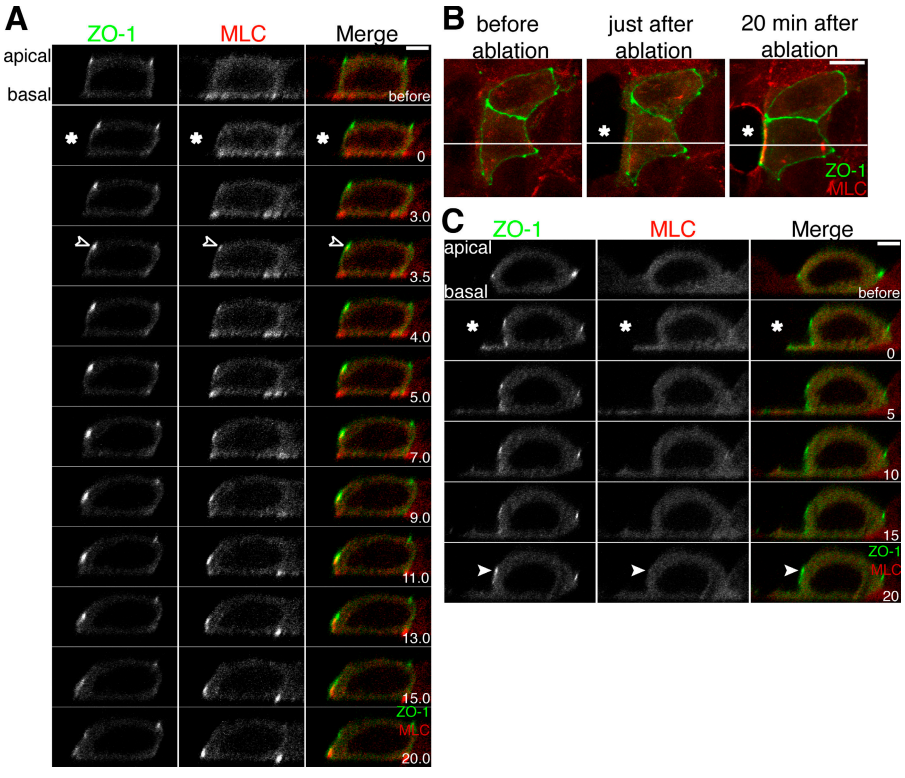

Figure 4. **The myosin ring forms at the tight junction.** (A) Cells in a monolayer of MLC-RFP cells transiently expressing ZO-1–EGFP were ablated, and XZ images were collected. MLC-RFP started to accumulate at site containing ZO-1–EGFP concentration (open arrowheads), and the two moved together thereafter. (B) Z stacks of XY sections taken before and after ablation were projected along the Z axis, and images of MLC-RFP (red) and ZO-1-EGFP (green) were merged. (C) Cells were treated and observed as in A in the presence of Y27632. MLC-RFP accumulation at the apical–lateral border was attenuated, and ZO-1–EGFP concentration remained at the initial position (closed arrowheads). Asterisks indicate the ablated cells. Bars: (B) 10 µm; (A and C) 5 µm.

Rho-kinase accumulates at the apical–lateral border of cells surrounding a wound

Because Rho-kinase is required for wound closure, we examined its localization during this process. Previous studies have shown that Rho-kinase is distributed in the cytoplasm (Matsui et al., 1996) but is localized specifically at the cleavage furrow during cytokinesis (Kosako et al., 1999) and along actin stress fibers (Kawabata et al., 2004) and vimentin intermediate filaments (Sin et al., 1998). EGFP–Rho-kinase, coexpressed with MLC-RFP, distributed diffusely in the cytoplasm and was not found with MLC-RFP at the base of cells within the intact monolayer (Fig. 3 B and not depicted). Expression of EGFP–Rho-kinase did not affect the localization of MLC-RFP. After laser ablation, EGFP–Rho-kinase accumulated simultaneously with MLC-RFP at the apical–lateral border facing the wound and then moved with MLC-RFP toward the base of the cell; meanwhile, coaccumulation of EGFP–Rho-kinase and MLC-RFP was not observed in the basal–lateral border (Fig. 3, A and C).

It is unknown why the accumulation of Rho-kinase was observed only at the apical–lateral border and not at the basal–lateral border, whereas Rho-kinase activity was involved at both sites during wound closure. Because Y27632 inhibited MLC ring accumulation (Fig. 2 B), it is possible that Rho-kinase locally activates actomyosin ring assembly at that site by phosphorylating coaccumulated MLC. That Rho-kinase colocalized and moved with the actomyosin ring during wound closure suggests that Rho-kinase also plays a role in maintaining contractile activity of the actomyosin ring. These results might be correlated with the observation of a concentric Rho active zone around wounds in *Xenopus laevis* oocytes and its movement inward in concert with wound closure (Benink and Bement, 2005).

The myosin ring forms at the tight junction

Our results show that the actomyosin ring and its activator Rho-kinase colocalize at the apical–lateral border of cells. This region of the plasma membrane of polarized epithelial cells contains many junctional complexes that constitute the tight junction and adherens junction. A previous report demonstrated that the tight junction scaffolding protein ZO-1 colocalized with actin filaments in the ring 1 h after wounding (Bement et al., 1993). To examine at which sites the actomyosin ring was organized and the dynamics of its localization, we compared the distribution of junctional proteins with the distribution of MLC in the apical–lateral region.

In a cell expressing both MLC-RFP and ZO-1–EGFP, MLC-RFP started to accumulate at the site of ZO-1–EGFP concentration adjacent to the ablated cells within 5 min of ablation, and the two comigrated thereafter (Fig. 4, A and B). As shown in Fig. 5 A, MLC accumulated slightly above the tip of E-cadherin or α-catenin signal but below claudin-1 and did not precisely colocalize with either of them, yet MLC accumulation colocalized with l-afadin at the apical–lateral border. Note that in MDCK cells the adherens junction is poorly developed and the major component of adherens junctions, E-cadherin, is localized over the entire surface of the lateral membrane and is not focused in an adherens junction (Vogelmann and Nelson, 2005).

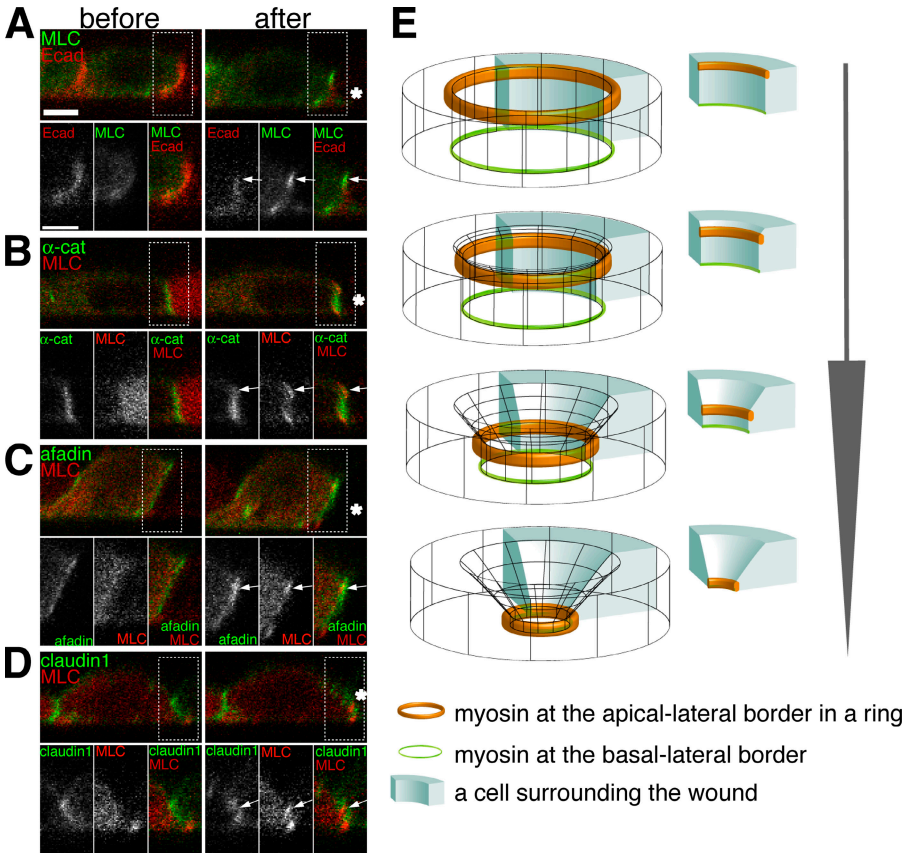

Figure 5. **Comparison between distribution of junctional proteins and distribution of MLC after ablation.** (A–D) XZ sections of MLC-EGFP cells expressing Ecad-RFP (A) and MLC-RFP cells expressing EGFP–α-catenin (B), EGFP–l-afadin (C), or EGFP-claudin1 (D) were observed before (left) and after (right) ablation. Bottom panels show the boxed regions of the top panel at higher magnification. Arrows indicate the sites of MLC accumulation at the apical–lateral border. Asterisks indicate the ablated cells. Bars, 5 μm. (E) Diagram of myosin accumulation and its dynamics during wound closure.

Significantly, addition of Y27632 caused ZO-1–EGFP to remain at its initial position, and as shown previously, there was little or no accumulation of MLC or change in cell shape for 20 min after ablation (Fig. 4 C). These data suggest that a complex including ZO-1 and l-afadin localized at the cytoplasmic surface of tight junction strands serves as a scaffold for assembly and localization of the myosin ring adjacent to the wound. Although the molecular linkages involved are not fully understood, ZO-1 and l-afadin have been reported to link the actin cytoskeleton to tight junction strands and nectin, respectively (Tsukita et al., 2001; Takai and Nakanishi, 2003); therefore, ZO-1/claudin and l-afadin/nectin are good candidates to anchor the actomyosin cables to cell–cell adhesion sites around the wound to form a continuous ring.

Our results reveal a tight spatiotemporal coordination between localized recruitment of Rho-kinase and myosin, activation of actomyosin contraction, and dramatic cell shape changes to close the wound by two fundamentally different mechanisms. First, actomyosin assembly and contraction draw adjacent apical edges in and down, and second, lamellipodial protrusions extend into the wound independent of contraction but regulated by Rho-kinase. Further analysis to define the mechanisms regulating Rho-kinase localization and activation at each site is critical to clarify how cells integrate biochemical and mechanical signals to reorganize the cytoskeleton. In addition, the relationship between cytoskeletal reorganization and remodeling of cell–cell adhesions needs to be clarified to understand the morphological changes that close wounds in epithelial sheets.

Materials and methods

Plasmids

For the MLC-EGFP construct, chicken *MLC* cDNA (Komatsu et al., 2000; a gift from M. Ikebe, University of Massachusetts Medical School, Worcester, MA) was amplified by PCR and subcloned into pEGFP-N3 (pEGFP-N3-MLC). For the MLC-RFP construct, *monomeric RFP of Discosoma* cDNA was amplified by PCR and cloned in place of *EGFP* cDNA in pEGFP-N3-MLC. The EGFP–Rho-kinase construct was provided by K. Kaibuchi (Nagoya University Graduate School of Medicine, Nagoya, Japan). pCYFP-ZO-1 and pNYFP-Cld1 (Matsuda et al., 2004) were provided by S. Tsukita (deceased). For ZO-1–EGFP and EGFP-Claudin1, *ZO-1* and *Claudin1* cDNA were cloned into pCAG-CGFP and -NGFP, respectively. The EGFP–l-afadin construct was provided by Y. Takai (Osaka University Graduate School of Medicine, Suita, Japan; Sato et al., 2006). The EYFP-C3 toxin construct was provided by E. Lemichez (Institut National de la Santé et de la Recherche Médicale, Nice, France).

Chemicals

Blebbistatin, Y27632, and ML-7 were purchased from Calbiochem.

Cells and transfection

MDCKII cells expressing Ecad-RFP, EGFP–α-catenin (Yamada et al., 2005), or EGFP-actin (Ehrlich et al., 2002) were maintained in DME supplemented with 10% fetal bovine serum. MDCKII cells expressing MLC were maintained in DME supplemented with 10% calf serum. For live-cell imaging, we used complete medium buffered with 20 mM Hepes, pH 7.4. Plasmid transfection was performed with Lipofectamine 2000 (Invitrogen) or Nucleofector (Amaxa Biosystems) according to the manufacturer's protocol. To isolate MDCKII cells stably expressing MLC-EGFP, MLC-RFP, or Ecad-RFP, cells were transfected with respective plasmid and clones were selected using G-418 (Invitrogen).

Laser ablation of cells

To ablate cells, we used an ultraviolet laser as described previously (Kiehart et al., 2000), a N_2 laser (model VSL-337ND; Laser Science, Inc.) that produced 3-ns pulses of 6 μJ (at the source) of a 337.1-nm UV light mounted on a microscope (IX70; Olympus). The laser beam was directed onto a dichroic mirror (380DCLP; Chroma Technology Corp.) and passed through the objective (UApo/340, 40×; Olympus) onto the specimen. The dose of UV light delivered was adjusted by counting the number of pulses at 2 Hz. The laser was focused onto the cell to be ablated and activated while under bright field observation. One to three cells were ablated in each experiment.

Time-lapse imaging

Confluent monolayers of cells were grown on glass coverslips coated with collagen (type I; Sigma-Aldrich) for 24–48 h and laser ablated. Images of cells were collected at 37°C with a microscope (40×/1.35 NA, oil-immersion objective; Olympus) through a cooled charge-coupled device camera (CoolSNAP HQ; Roper Scientific, Inc.) using Simple PCI software (Compix, Inc.) or with a confocal microscope (Fluoview 300; PlanApo; 60×/1.4 NA; oil-immersion objective; Olympus) configured on a microscope with Fluoview 2.1 software for 15–60 min at 30–60-s intervals. XZ images were collected at 30-s intervals. Image analysis was done with the open-source program ImageJ (NIH).

Immunofluorescence

After laser ablation, cells were maintained at 37°C for the indicated time and fixed in 3.7% (vol/vol) formaldehyde in PBS. Fixed cells were permeabilized with 0.2% Triton X-100 in PBS for 10 min and incubated with anti–phospho-MLC (Thr18/Ser19) antibody (Cell Signaling) followed by detection with Alexa Fluor 568 anti-rabbit secondary antibody (Invitrogen). Cells were incubated with Alexa Fluor 568 phalloidin (Invitrogen) to visualize F-actin.

Online supplemental material

Fig. S1 shows the extrusion of laser-ablated cells by surrounding cells and F-actin ring around the ablated cell. Fig. S2 shows that ML-7 had little or no effect on either the MLC-EGFP accumulation or the ensuing cell shape changes. Video 1 is a time-lapse video of Ecad-RFP. Video 2 is a time-lapse video of MLC-EGFP. Video 3 is a time-lapse video of MLC-EGFP. Video 4 is a time-lapse video of MLC-EGFP in XZ sections showing cells at both sides of the wound. Video 5 is a time-lapse video of MLC-EGFP with Y27632. Video 6 is a time-lapse video of EGFP–Rho-kinase. Video 7 is a time-lapse video of MLC-RFP. Video 8 is a time-lapse video of ZO-1–EGFP. Video 9 is a time-lapse video of MLC-RFP.

We thank M. Ikebe, K. Kaibuchi, E. Lemichez, and S. Tsukita for providing materials; M. Furuse for consistent support; and Y. Takai for providing materials and support. We also thank all the members of the Sheetz laboratory for their kind cooperation.

T.D. Perez was supported by a predoctoral fellowship from the Howard Hughes Medical Institute. This work was supported by National Institutes of Health grants RO1 EB001480 to M.P. Sheetz and RO1 GM35227 to W.J. Nelson.

Submitted: 18 September 2006
Accepted: 1 December 2006

References

Bement, W.M., P. Forscher, and M.S. Mooseker. 1993. A novel cytoskeletal structure involved in purse string wound closure and cell polarity maintenance. *J. Cell Biol.* 121:565–578.

Benink, H.A., and W.M. Bement. 2005. Concentric zones of active RhoA and Cdc42 around single cell wounds. *J. Cell Biol.* 168:429–439.

Bertet, C., L. Sulak, and T. Lecuit. 2004. Myosin-dependent junction remodelling controls planar cell intercalation and axis elongation. *Nature.* 429:667–671.

Ehrlich, J.S., M.D. Hansen, and W.J. Nelson. 2002. Spatio-temporal regulation of Rac1 localization and lamellipodia dynamics during epithelial cell-cell adhesion. *Dev. Cell.* 3:259–270.

Ikebe, M., and D.J. Hartshorne. 1985. Phosphorylation of smooth muscle myosin at two distinct sites by myosin light chain kinase. *J. Biol. Chem.* 260:10027–10031.

Kawabata, S., J. Usukura, N. Morone, M. Ito, A. Iwamatsu, K. Kaibuchi, and M. Amano. 2004. Interaction of Rho-kinase with myosin II at stress fibres. *Genes Cells.* 9:653–660.

Kiehart, D.P., C.G. Galbraith, K.A. Edwards, W.L. Rickoll, and R.A. Montague. 2000. Multiple forces contribute to cell sheet morphogenesis for dorsal closure in *Drosophila*. *J. Cell Biol.* 149:471–490.

Komatsu, S., T. Yano, M. Shibata, R.A. Tuft, and M. Ikebe. 2000. Effects of the regulatory light chain phosphorylation of myosin II on mitosis and cytokinesis of mammalian cells. *J. Biol. Chem.* 275:34512–34520.

Kosako, H., H. Goto, M. Yanagida, K. Matsuzawa, M. Fujita, Y. Tomono, T. Okigaki, H. Odai, K. Kaibuchi, and M. Inagaki. 1999. Specific accumulation of Rho-associated kinase at the cleavage furrow during cytokinesis: cleavage furrow-specific phosphorylation of intermediate filaments. *Oncogene.* 18:2783–2788.

Martin, P., and J. Lewis. 1992. Actin cables and epidermal movement in embryonic wound healing. *Nature.* 360:179–183.

Martin, P., and S.M. Parkhurst. 2004. Parallels between tissue repair and embryo morphogenesis. *Development.* 131:3021–3034.

Matsuda, M., A. Kubo, M. Furuse, and S. Tsukita. 2004. A peculiar internalization of claudins, tight junction-specific adhesion molecules, during the intercellular movement of epithelial cells. *J. Cell Sci.* 117:1247–1257.

Matsui, T., M. Amano, T. Yamamoto, K. Chihara, M. Nakafuku, M. Ito, T. Nakano, K. Okawa, A. Iwamatsu, and K. Kaibuchi. 1996. Rho-associated kinase, a novel serine/threonine kinase, as a putative target for small GTP binding protein Rho. *EMBO J.* 15:2208–2216.

Nikolaidou, K.K., and K. Barrett. 2004. A Rho GTPase signaling pathway is used reiteratively in epithelial folding and potentially selects the outcome of Rho activation. *Curr. Biol.* 14:1822–1826.

Rosenblatt, J., M.C. Raff, and L.P. Cramer. 2001. An epithelial cell destined for apoptosis signals its neighbors to extrude it by an actin- and myosin-dependent mechanism. *Curr. Biol.* 11:1847–1857.

Russo, J.M., P. Florian, L. Shen, W.V. Graham, M.S. Tretiakova, A.H. Gitter, R.J. Mrsny, and J.R. Turner. 2005. Distinct temporal-spatial roles for rho kinase and myosin light chain kinase in epithelial purse-string wound closure. *Gastroenterology.* 128:987–1001.

Sato, T., N. Fujita, A. Yamada, T. Ooshio, R. Okamoto, K. Irie, and Y. Takai. 2006. Regulation of the assembly and adhesion activity of E-cadherin by nectin and afadin for the formation of adherens junctions in Madin-Darby canine kidney cells. *J. Biol. Chem.* 281:5288–5299.

Shelton, C.A., J.C. Carter, G.C. Ellis, and B. Bowerman. 1999. The nonmuscle myosin regulatory light chain gene mlc-4 is required for cytokinesis, anterior-posterior polarity, and body morphology during *Caenorhabditis elegans* embryogenesis. *J. Cell Biol.* 146:439–451.

Sin, W.C., X.Q. Chen, T. Leung, and L. Lim. 1998. RhoA-binding kinase alpha translocation is facilitated by the collapse of the vimentin intermediate filament network. *Mol. Cell. Biol.* 18:6325–6339.

Takai, Y., and H. Nakanishi. 2003. Nectin and afadin: novel organizers of intercellular junctions. *J. Cell Sci.* 116:17–27.

Tsukita, S., M. Furuse, and M. Itoh. 2001. Multifunctional strands in tight junctions. *Nat. Rev. Mol. Cell Biol.* 2:285–293.

Vogelmann, R., and W.J. Nelson. 2005. Fractionation of the epithelial apical junctional complex: reassessment of protein distributions in different substructures. *Mol. Biol. Cell.* 16:701–716.

Wood, W., A. Jacinto, R. Grose, S. Woolner, J. Gale, C. Wilson, and P. Martin. 2002. Wound healing recapitulates morphogenesis in *Drosophila* embryos. *Nat. Cell Biol.* 4:907–912.

Yamada, S., S. Pokutta, F. Drees, W.I. Weis, and W.J. Nelson. 2005. Deconstructing the cadherin-catenin-actin complex. *Cell.* 123:889–901.

Young, P.E., A.M. Richman, A.S. Ketchum, and D.P. Kiehart. 1993. Morphogenesis in *Drosophila* requires nonmuscle myosin heavy chain function. *Genes Dev.* 7:29–41.

Zallen, J.A., and E. Wieschaus. 2004. Patterned gene expression directs bipolar planar polarity in *Drosophila*. *Dev. Cell.* 6:343–355.